

Spin-orbit state selective formation of rare gas chlorides from threebody ionic recombination reactions of $Rg+(2 P 1/2,3/2)+Cl^-+He$ at thermal energy

Masaharu Tsuji, Makoto Furusawa, Hiroyuki Kouno, and Yukio Nishimura

Citation: *The Journal of Chemical Physics* **94**, 4291 (1991); doi: 10.1063/1.460615

View online: <http://dx.doi.org/10.1063/1.460615>

View Table of Contents: <http://scitation.aip.org/content/aip/journal/jcp/94/6?ver=pdfcov>

Published by the [AIP Publishing](#)

Articles you may be interested in

Formation of $ArCl(B,C)$, $Ar(3 P 2)$, and Cl^* by the threebody ionic recombination reaction of $Ar+(2 P 3/2)+Cl^-+Ar$

J. Chem. Phys. **101**, 328 (1994); 10.1063/1.468193

Formation of $ArCl(B,C)$, $Ar(3 P 2)$, and Cl^* by the threebody ionic recombination reaction of $Ar+(2 P 3/2)+Cl^-+He$

J. Chem. Phys. **99**, 1710 (1993); 10.1063/1.465288

Comparison of the $Rg+(2 P 1/2)/Cl^-/He$ and $Rg+(2 P 3/2)/Cl^-/He$ threebody ionic recombination reactions for the formation of $RgCl^*$, Rg^* , and Cl^*

J. Chem. Phys. **97**, 1079 (1992); 10.1063/1.463287

Spin-orbit state selectivity in KrF^* and XeF^* formation from ion recombination reactions of $Kr+(2 P 3/2,1/2)$ and $Xe+(2 P 3/2,1/2)$ with SF_6^- in the flowing afterglow

J. Chem. Phys. **92**, 6502 (1990); 10.1063/1.458284

Spin-orbit state selected reactions of $Kr+(2 P 3/2)$ and $2 P 1/2)$ with H_2 , D_2 , and HD from thermal energies to 20 eV c.m.

J. Chem. Phys. **85**, 6380 (1986); 10.1063/1.451469



Spin-orbit state selective formation of rare gas chlorides from three-body ionic-recombination reactions of $\text{Rg}^+ (^2P_{1/2,3/2}) + \text{Cl}^- + \text{He}$ at thermal energy

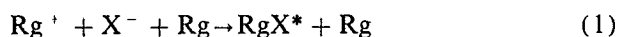
Masaharu Tsuji, Makoto Furusawa, Hiroyuki Kouno, and Yukio Nishimura
Institute of Advanced Material Study and Department of Molecular Science and Technology,
Graduate School of Engineering Sciences, Kyushu University, Kasuga-shi, Fukuoka 816, Japan

(Received 10 September 1990; accepted 5 December 1990)

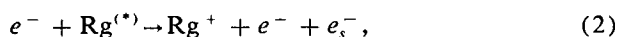
The $\text{ArCl}(C-A)$, $\text{KrCl}(B-X, C-A, D-X)$, and $\text{XeCl}(B-X, C-A, D-X)$ emissions have been observed from ionic-recombination reactions of Rg^+ ($\text{Rg} = \text{Ar}, \text{Kr}, \text{or Xe}$) with Cl^- in the flowing afterglow. Positive Rg^+ ions are formed by $\text{He}(2^3S)/\text{Rg}$ Penning ionization, while negative Cl^- ions are produced through thermal electron attachment to CCl_4 . The dependence of RgCl^* emission intensities on the buffer He gas pressure indicates that the excimer emissions arise from three-body reactions of $\text{Rg}^+ + \text{Cl}^- + \text{He}$. The spin-orbit state selectivity in the KrCl^* and XeCl^* formation is studied by isolating one of the spin-orbit levels of Rg^+ , $^2P_{1/2}$ or $^2P_{3/2}$. Although the $\text{Kr}^+(^2P_{1/2})$ reaction provides the $\text{KrCl}(B-X, C-A, D-X)$ emissions with $B:C:D$ distribution of $0.19 \pm 0.02:0.12 \pm 0.01:0.69 \pm 0.04$, only $\text{XeCl}(D-X)$ emission is observed from the $\text{Xe}^+(^2P_{1/2})$ reaction. The $\text{Kr}^+(^2P_{3/2})$ and $\text{Xe}^+(^2P_{3/2})$ reactions give the $\text{RgCl}(B-X, C-A)$ emissions with $B:C$ branching ratios of $0.60 \pm 0.06:0.40 \pm 0.04$ for KrCl^* and $0.62 \pm 0.06:0.38 \pm 0.04$ for XeCl^* . The high propensities for the D formation from the $\text{Rg}^+(^2P_{1/2})$ reactions and for the B and C formation from the $\text{Rg}^+(^2P_{3/2})$ reactions suggest that $\text{Rg}^+(^2P_{1/2}) + \text{Cl}^-$ and $\text{Rg}^+(^2P_{3/2}) + \text{Cl}^-$ characters are conserved well for the formation of RgCl^* in the three-body ionic-recombination reactions. The relative formation rate of $\text{RgCl}(D)$ from the $\text{Rg}^+(^2P_{1/2})$ reaction to that of $\text{RgCl}(B,C)$ from the $\text{Rg}^+(^2P_{3/2})$ reaction was estimated to be 0.14 ± 0.02 for KrCl^* and 0.033 ± 0.006 for XeCl^* . The slower $\text{RgCl}(D)$ formation rates are attributed to fast predissociation of $[\text{Rg}^+(^2P_{1/2})\text{Cl}^-]^*$ intermediates into $\text{Rg}^* + \text{Cl}$ and/or $\text{Rg} + \text{Cl}^*$ than that of $[\text{Rg}^+(^2P_{3/2})\text{Cl}^-]^*$ ones.

I. INTRODUCTION

The three-body ionic-recombination process



plays an important role for the population of the emitting excited states of rare gas monohalide (RgX^*) in rare gas-halogen laser system operated at high pressure (1/2–5 atm).^{1–5} Rg^+ ions are produced by electron-impact ionization of rare gas atoms in the ground and metastable states:



while negative X^- ions are formed by dissociative electron attachment of the slow electrons ejected in reaction (2):



In the previous e -beam experiments, various mixtures of a rare gas and a halogen donor were irradiated by a high energy e -beam pulse for the generation of rare gas excimer. Since complicated pumping and quenching reactions simultaneously occur in the e -beam experiments, its application to the detailed dynamical analysis of the three-body ionic-recombination processes is difficult.

Recently, we have successfully applied the flowing afterglow (FA) apparatus to the study on two-body dissociative ionic-recombination reactions^{6,7}



where Rg represents Ar, Kr, or Xe. Positive Rg^+ ions were formed by $\text{He}(2^3S)/\text{Rg}$ Penning ionization and negative

SF_6^- ions were produced by attachment of Penning electrons to SF_6 . The spin-orbit state selectivity in the KrF^* and XeF^* formation was examined by selecting one of the spin-orbit levels of Kr^+ and Xe^+ , $^2P_{1/2}$ or $^2P_{3/2}$. It was found that Kr^+ and Xe^+ ions in the $^2P_{1/2}$ level preferentially give the D state, while those in the $^2P_{3/2}$ level give only the B and C states. The high spin-orbit state selectivity was explained by the conservation of $\text{Rg}^+(^2P_{3/2}) + \text{F}^-$ and $\text{Rg}^+(^2P_{3/2}) + \text{F}^-$ characters.

Here, our FA study on ionic-recombination reactions was extended to the formation of RgCl^* ($\text{Rg} = \text{Ar}, \text{Kr}, \text{or Xe}$) by the following three-body reaction:



The effect of incident spin-orbit state on the excimer formation was examined for KrCl^* and XeCl^* by isolating Kr^+ and Xe^+ in the $^2P_{1/2}$ or $^2P_{3/2}$ level. The spin-orbit state selectivity is discussed from the potential energy diagram. The relative formation rate constants of $\text{RgCl}(D)$ to those of $\text{RgCl}(B,C)$ were estimated by reference to $\text{RgF}(D)/\text{RgF}(B)$ ratios in reaction (4).

II. EXPERIMENTAL

A schematic diagram of the FA apparatus used in this study is shown in Fig. 1. The FA apparatus consists of a stainless steel main flow tube (i.d. 60 mm) and a quartz discharge tube (i.d. 12 mm). The carrier He gas was passed through a microwave discharge to form active species of He

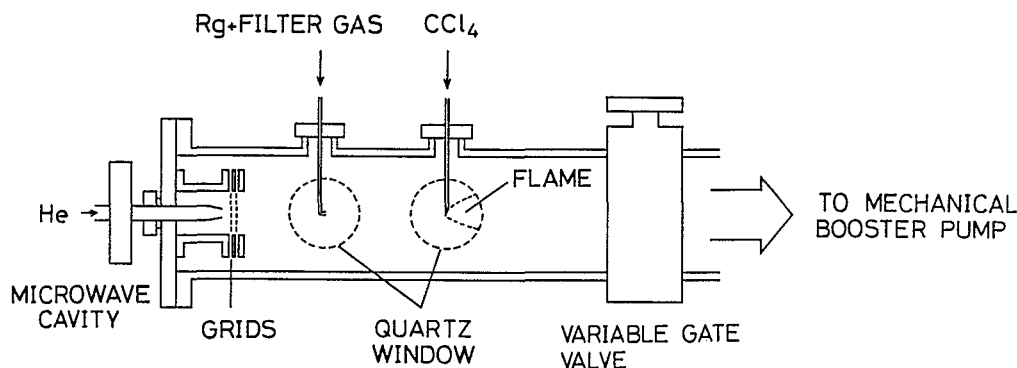
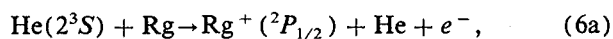


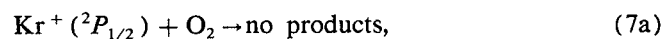
FIG. 1. Schematic of the flowing afterglow apparatus used for three-body ionic-recombination reactions of $\text{Rg}^+ + \text{Cl}^- + \text{He}$.

[$\text{He}(2^3S)$, He^+ , and He_2^+]. To obtain the only metastable $\text{He}(2^3S)$ atoms, ionic active species were removed from the discharge flow by using a pair of ion-collector grids. A small amount of Rg (Ar, Kr, or Xe) was injected into the He discharge flow from the first gas inlet placed 10 cm downstream from the center of the microwave discharge. The $\text{Rg}^+(^2P_{1/2,3/2})$ ions were generated by $\text{He}(2^3S)$ Penning ionization of Rg:



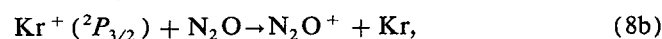
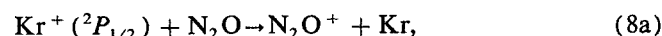
The formation rate constants of $\text{Ar}^+(^2P_{1/2,3/2})$, $\text{Kr}^+(^2P_{1/2,3/2})$, and $\text{Xe}^+(^2P_{1/2,3/2})$ have been measured as (7–9), (10–14), and (12–18) $\times 10^{-11} \text{cm}^3 \text{s}^{-1}$, respectively, with a statistical branching fraction of ~ 2 for reactions (6b)/(6a).^{8,9} Under operating conditions, only $\text{Ar}^+(^2P_{3/2})$ is present due to relaxation of $\text{Ar}^+(^2P_{1/2})$ by superelastic collisions with electrons,^{10–13} whereas the presence of both spin-orbit states was confirmed for Kr^+ and Xe^+ by observing the $\text{KrF}(B-X, D-X)$ and $\text{XeF}(B-X, D-X)$ emissions from reaction (4). CCl_4 was added from the second inlet placed 10 cm further downstream. The partial pressure in the reaction zone was 0.3–20 Torr (1 Torr = 133.3 Pa) for He, 3–40 mTorr for Ar, Kr, or Xe, and 5–15 mTorr for CCl_4 . High He pressure experiments above 1.5 Torr were carried out by closing a variable gate valve.

When the effect of incident spin-orbit states in Kr^+ and Xe^+ was examined, one of the spin-orbit states was isolated before reaching the second gas inlet. For the isolation of $\text{Kr}^+(^2P_{1/2})$, $\text{Xe}^+(^2P_{1/2})$, and $\text{Xe}^+(^2P_{3/2})$, O_2 or N_2O , C_2H_2 , and CH_4 were used as filter gases, respectively, because the quenching rate constants of the $^2P_{1/2}$ and $^2P_{3/2}$ states are different at least 1 order of magnitude¹⁴:



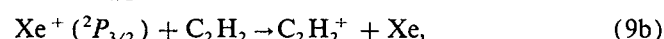
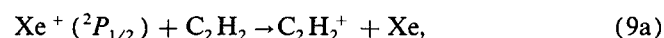
$$k_{7a} < 1 \times 10^{-12} \text{cm}^3 \text{s}^{-1},$$

$$k_{7b} = 4.7 \times 10^{-11} \text{cm}^3 \text{s}^{-1},$$



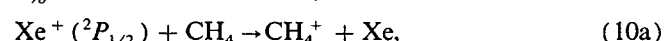
$$k_{8a} = 1.5 \times 10^{-11} \text{cm}^3 \text{s}^{-1},$$

$$k_{8b} = 4.0 \times 10^{-10} \text{cm}^3 \text{s}^{-1},$$



$$k_{9a} = 3.5 \times 10^{-11} \text{cm}^3 \text{s}^{-1},$$

$$k_{9b} = 5.0 \times 10^{-10} \text{cm}^3 \text{s}^{-1},$$



$$k_{10a} = 9.0 \times 10^{-10} \text{cm}^3 \text{s}^{-1},$$

$$k_{10b} < 1 \times 10^{-12} \text{cm}^3 \text{s}^{-1}.$$

These filter gases were premixed with a rare gas and injected from the first gas inlet. The partial pressures of the filter gases were 30–200 mTorr. Although no appropriate filter gas has been known for the $\text{Kr}^+(^2P_{3/2})$ productions, its isolation could be achieved by collisional relaxation from $^2P_{1/2}$ to $^2P_{3/2}$ at high Kr gas pressures.

The RgCl^* emission spectra were observed through a quartz window attached to the main flow tube. Observations in the 190–600 nm region were made with a Jarrell Ash 1 m monochromator equipped with a Hamamatsu Photonics R376 photomultiplier. The output signal of the photomultiplier tube was processed with a dc amplifier and displayed on a strip chart recorder. The detection system was calibrated in the ultraviolet with a standard D_2 lamp and in the visible with a standard halogen lamp.

III. RESULTS AND DISCUSSION

A. Excitation processes of RgCl^* excimers

Figures 2(a)–4(a) show typical emission spectra resulting from reactions of the metastable $\text{Ar}(^3P_{2,0})$, $\text{Kr}(^3P_2)$, and $\text{Xe}(^3P_2)$ atoms with CCl_4 . $\text{Ar}(^3P_{2,0})$ and $\text{Kr}(^3P_2)$ were generated by a microwave discharge of the pure Ar and Kr gases operated at 0.15 Torr for Ar and 35 mTorr for Kr, whereas $\text{Xe}(^3P_2)$ was obtained by the microwave discharge of a 1:50 mixture of Xe:Ar operated at a total pressure of 0.10 Torr. The $\text{ArCl}(C-A)$, $\text{KrCl}(B-X, C-A)$, and $\text{XeCl}(B-X, B-A, C-A)$ emissions are identified together with $\text{Cl}_2(D'-A')$ and $\text{CCl}(A-X)$ in agreement with the previous findings of Setser and his co-workers^{15–20} and Golde and Poletti.²¹ These excimers are excited by the chemiluminescent reactions

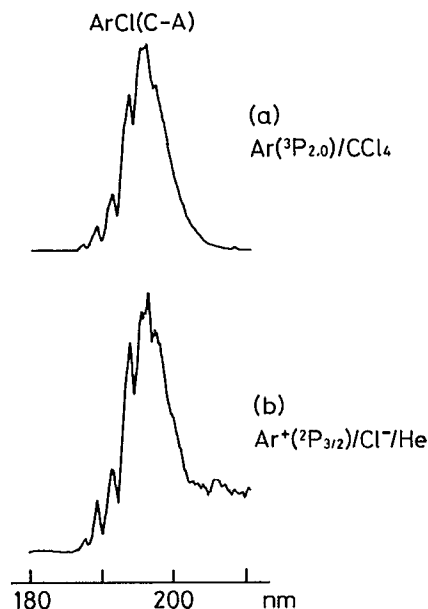
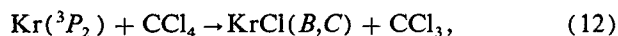
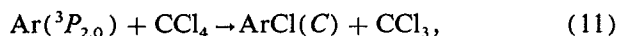


FIG. 2. ArCl^* emission produced from (a) the $\text{Ar}(^3P_{2,0}) + \text{CCl}_4$ reaction in the Ar afterglow and (b) the $\text{Ar}^+(^2P_{3/2}) + \text{Cl}^- + \text{He}$ reaction in the He afterglow at a He pressure of 3.0 Torr (uncorrected for spectral response). Oscillatory structure in the 190–200 nm region is due to absorption of O_2 . Optical resolution was 3.8 Å.



It has been believed that the RgCl^* excimers are formed through the harpoon-type reaction via $[\text{Rg}^+ \text{CCl}_4^-]$ intermediates¹⁸

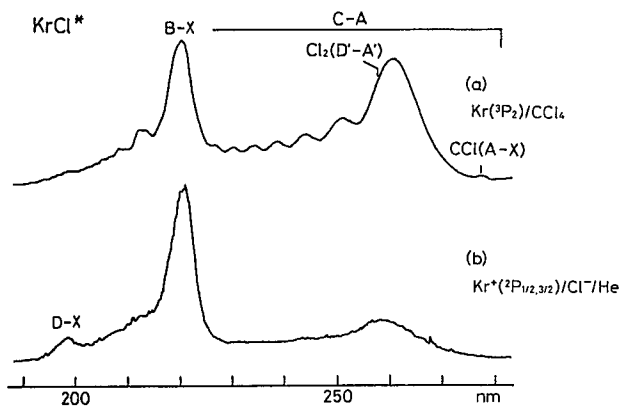
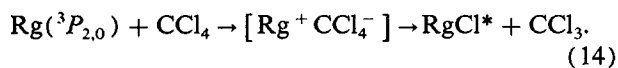


FIG. 3. KrCl^* emission produced from (a) the $\text{Kr}(^3P_2) + \text{CCl}_4$ reaction in the Kr afterglow and (b) the $\text{Kr}^+(^2P_{1/2,3/2}) + \text{Cl}^- + \text{He}$ reaction in the He afterglow at a He pressure of 1.8 Torr (uncorrected for spectral response). Optical resolution was 4.7 Å.

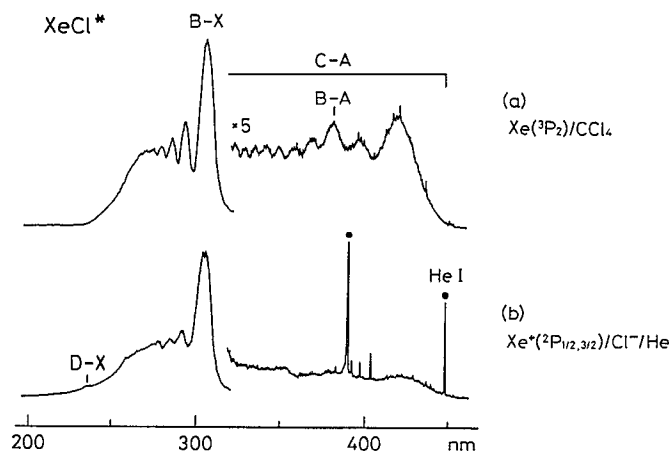
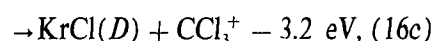
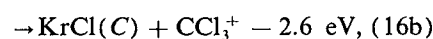
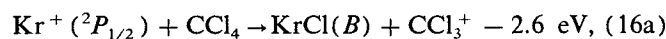
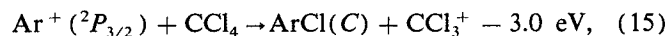
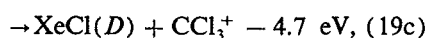
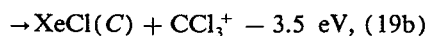
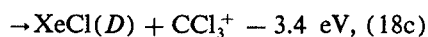
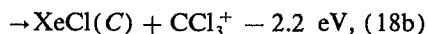
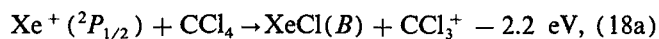
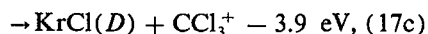
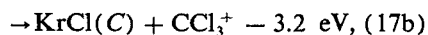
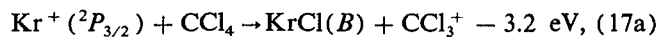


FIG. 4. XeCl^* emission produced from (a) the $\text{Xe}(^3P_2) + \text{CCl}_4$ reaction in the Ar/Xe afterglow and (b) the $\text{Xe}^+(^2P_{1/2,3/2}) + \text{Cl}^- + \text{He}$ reaction in the He afterglow at a He pressure of 5.7 Torr (uncorrected for spectral response). Optical resolution was 4.7 Å.

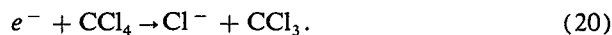
When small amounts of Rg (Ar, Kr, or Xe) and CCl_4 are added into the He discharge flow through the first and second gas inlets, respectively, RgCl^* emissions are also detected as shown in Figs. 2(b)–4(b). In addition to the $\text{ArCl}(C-A)$, $\text{KrCl}(B-X, C-A)$, and $\text{XeCl}(B-X, C-A)$ emissions observed in the $\text{Rg}(^3P_{2,0})/\text{CCl}_4$ reactions, weak $\text{KrCl}(D-X)$ and $\text{XeCl}(D-X)$ emissions²² are found on the short wavelength side of the $\text{KrCl}(B-X)$ and $\text{XeCl}(B-X)$ main bands. The spectral features of $\text{KrCl}(B-X, C-A)$ are different from those resulting from the $\text{Kr}(^3P_2)/\text{CCl}_4$ reaction (Fig. 3). Although typical oscillatory structure due to bound–free emission from highly vibrationally excited states is found in Fig. 3(a), it is either weak or absent in Fig. 3(b). The $B-X/C-A$ intensity ratio in Fig. 3(b) is larger than that in Fig. 3(a). Similar differences are found for the oscillatory structure of $\text{XeCl}(C-A)$ and the $B-X/C-A$ intensity ratio of XeCl^* (Fig. 4). However, the $\text{XeCl}(B-X)$ emission gives a similar oscillatory pattern as found in the $\text{Xe}(^3P_2)/\text{CCl}_4$ reaction.

Total quenching cross sections of $\text{He}(2^3S)$ by Ar, Kr, and Xe at 300 K have been determined to be 5–10, 8–10, and 10–14 Å², respectively.⁸ Since these values agree well with the total ionization cross sections of 7–23, 8, and 11 Å² for Ar, Kr, and Xe, respectively,⁸ Penning ionization leading to Rg^+ ions is the only product channel in the $\text{He}(2^3S)/\text{Rg}$ reaction. On the basis of Penning ionization electron spectra,⁹ all Rg^+ ions formed through process (6) are located in the ground $^2P_{1/2}$ and $^2P_{3/2}$ states. The $\text{Rg}^+(^2P_{1/2,3/2})/\text{CCl}_4$ ion–molecule reactions can be excluded from the possible excitation mechanism, because the excimer formation is endoergic based upon thermochemical and spectroscopic data:^{23–26}





where the ΔH_{298}° values for $\text{ArCl}(C)$ and $\text{KrCl}(B,C,D)$ are estimated assuming that their ground electronic states are flat and the energy separation between the B and C states of ArCl^* is zero by analogy with other rare gas halides.^{24,27,28} CCl_4 is a good thermal electron scavenger with a large electron attachment rate constant of $(3-4) \times 10^{-7} \text{ cm}^3 \text{ s}^{-1}$ at 300 K.²⁹ The thermal electron attachment to CCl_4 has been known to provide exclusively negative Cl^- ions²⁹



In the present experiment, Cl^- must be produced by attachment of Penning electrons to CCl_4 . Thus most probable excitation process of RgCl^* is either two-body or three-body ionic-recombination reaction as predicted in high-pressure electric discharge of mixtures of rare gases and halogen-containing compounds:^{1-5,30}



In an FA-mass spectroscopic study of Smith *et al.* on two-body ionic-recombination reactions of $\text{Rg}^+ (\text{Rg} = \text{Ar}, \text{Kr}, \text{or Xe}) + \text{X}^- (\text{X} = \text{F or Cl})$ at 300 K,³¹ no reaction was observed and the upper limits of the reaction rate constants were estimated to be $(0.2-1.0) \times 10^{-8} \text{ cm}^3 \text{ s}^{-1}$. On the other hand, rate constants of three-body ionic-recombination reactions $\text{Rg}^+ + \text{X}^- + \text{Rg}$ were theoretically evaluated to be $\sim 10^{-25} [\text{Rg}] \text{ cm}^3 \text{ s}^{-1}$.³² By using this value, the apparent two-body rate constant is expected to be the order of $10^{-8}-10^{-9} \text{ cm}^3 \text{ s}^{-1}$ at the present He buffer gas pressure range of 1-10 Torr. Actually, large apparent two-body rate constants of the order of $10^{-6}-10^{-7} \text{ cm}^3 \text{ s}^{-1}$ have been obtained for the three-body ionic-recombination reactions.^{2,33} Since the detection limit of two-body reactions in our FA apparatus is $\sim 10^{-15} \text{ cm}^3 \text{ s}^{-1}$, and the formation rate constant of Cl^- from electron attachment reaction (20) is large, these values are sufficient to observe the excimer emissions.

In order to determine whether RgCl^* emissions occur from the two-body or three-body reaction, the dependence of the emission intensity of RgCl^* on the He buffer gas pressure was compared with that of RgF^* from the two-body $\text{Rg}^+/\text{SF}_6^-$ reaction (4). Measurements were carried out by using a 1:12 mixture of $\text{SF}_6:\text{CCl}_4$ as a reagent. As an example, results for $\text{XeCl}(B-X)$ and $\text{XeF}(B-X)$ are shown in Fig. 5. The $\text{XeF}(B-X)$ emission appears at a He pressure of ~ 0.4 Torr, increases up to a peak at ~ 0.75 Torr, and slightly decreases in the 7.5-19 Torr range. The change in the $\text{XeF}(B-X)$ intensity with the He buffer gas pressure domin-

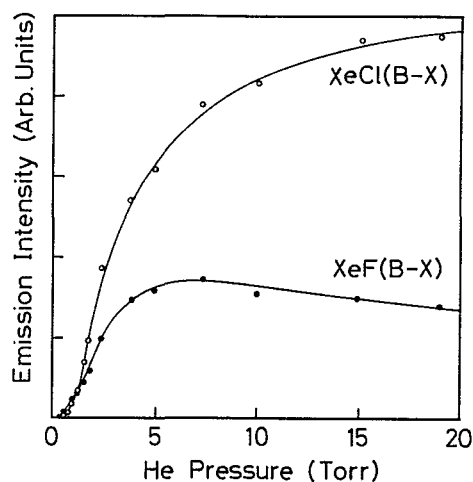
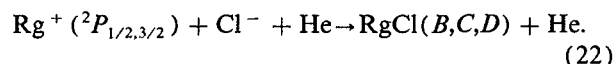
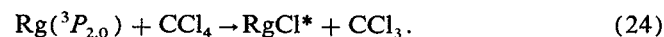
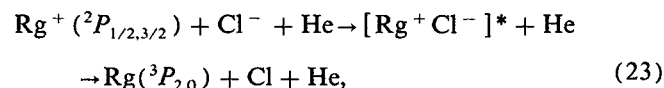


FIG. 5. Dependence of $\text{XeCl}(B-X)$ emission from $\text{Xe}^+ (^2P_{3/2}) + \text{Cl}^- + \text{He}$ and $\text{XeF}(B-X)$ emission from $\text{Xe}^+ (^2P_{3/2}) + \text{SF}_6^-$ on the He buffer gas pressure.

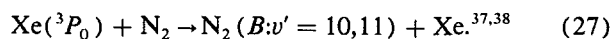
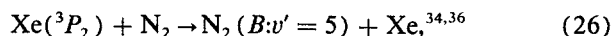
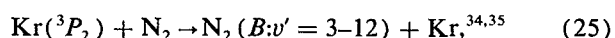
antly reflects variation of the concentration of $\text{He}(2^3S)$ which provides Xe^+ and slow electrons through process (6). The $\text{XeCl}(B-X)$ emission appears at a higher He pressure of ~ 0.7 Torr and the intensity increases more rapidly than for $\text{XeF}(B-X)$. No decrease in the $\text{XeCl}(B-X)$ intensity is found at the high pressure range. These results suggest that the buffer He atoms participate in the formation of $\text{XeCl}(B)$. A similar tendency was found for $\text{XeCl}(C,D)$, $\text{ArCl}(C)$, and $\text{KrCl}(B,C,D)$. From the above facts, it was concluded that the RgCl^* emissions result from the three-body ionic-recombination reactions at thermal energy:



There is a possibility that RgCl^* excimers do not arise from direct process (22), but an indirect process via predissociation of an $[\text{Rg}^+ \text{Cl}^-]^*$ intermediate into $\text{Rg}(^3P_{2,0}) + \text{Cl}$:



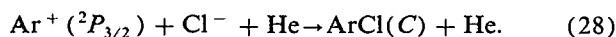
In order to examine such a possibility, N_2 was premixed with CCl_4 and $\text{N}_2(B-A)$ emission resulting from excitation transfer reactions of $\text{Kr}(^3P_2)$ and $\text{Xe}(^3P_{2,0})$ with N_2 was observed:



The absence of the $\text{N}_2(B-A)$ emission in the visible region led us to conclude that the above indirect processes are unimportant.

B. Spin-orbit state selectivity in the formation of $\text{RgCl}(B,C,D)$

Investigation of the ground $^2P_{1/2}$ and $^2P_{3/2}$ states of rare gas ions is part of a general concern about the reactivity of different spin-orbit states of reactant.³⁹ In the present study, the effect of spin-orbit states of $\text{Rg}^+ (^2P_{1/2,3/2})$ on the formation of RgCl^* was examined for Kr^+ and Xe^+ . Experiments for Ar^+ were not attempted, partly because only $\text{Ar}^+ (^2P_{3/2})$ is present under the operating conditions, and partly because $\text{ArCl}(B-X, D-X)$ emissions in the vacuum uv region are outside the present observation. The only finding about the spin-orbit state selectivity in the Ar^+ reaction is that the $\text{ArCl}(C-A)$ emission results from the $\text{Ar}^+ (^2P_{3/2})$ reaction:



This selectivity agrees with that found for the Kr^+ and Xe^+ reactions described below.

Figures 6(a)–6(c) show the KrCl^* spectra resulting from the three-body ionic-recombination reactions by $\text{Kr}^+ (^2P_{1/2,3/2})$, $\text{Kr}^+ (^2P_{1/2})$, and $\text{Kr}^+ (^2P_{3/2})$, respectively. The $\text{Kr}^+ (^2P_{1/2,3/2})$ spectrum measured without spin-orbit state selection consists of the $B(1/2)-X(1/2)$, $C(3/2)-A(3/2)$, and $D(1/2)-X(1/2)$ transitions of KrCl^* . When $\text{Kr}^+ (^2P_{1/2})$ was selected, an intense $D-X$ transition and weak $B-X$ and $C-A$ transitions are observed. On the other hand, a strong $B-X$ transition and a weak continuous $C-A$ transition are found by the $\text{Kr}^+ (^2P_{3/2})$ reaction. The $(B-X + C-A)/D-X$ ratio in the $\text{Kr}^+ (^2P_{1/2})$ reaction was independent of the O_2 filter gas pressure (0.08–0.2 Torr) and the He buffer gas pressure (1–20 Torr). Therefore, the contribution of residual $\text{Kr}^+ (^2P_{3/2})$ ions and collisional relaxation from D to B are expected to be unimportant for the $\text{KrCl}(B)$ formation. A similar slow electronic state transfer from D to B by collisions with the He buffer gas has recently been found by Yu and Setser in a $\text{Kr}(^3P_1)$ sensitization study on the relaxation and quenching of KrCl^* from the low-pressure collision-free limit up to ~ 5 atm pressure.²⁶ The radiative lifetime of $\text{KrCl}(B)$ τ_B is theoretically estimated to be 6 ns.⁴⁰ Although τ_D has not been reported to our best knowledge, it will be the same order of τ_B by analogy with other rare gas monohalides.^{24,27} The energy separation between the B and D states ΔE_{BD} is large ($\sim 5500 \text{ cm}^{-1}$). Therefore, the slow energy transfer from D to B is consequent of the short radiative lifetime of the D state and the large ΔE_{BD} separation. In contrast with the slow $D \rightarrow B$ energy transfer, Yu and Setser²⁶ found that the B and C states are collisionally mixed at high buffer gas pressures because of a long τ_C value of 87 ns and a small energy separation of $\Delta E_{BC} = E_C - E_B = 0 \pm 50 \text{ cm}^{-1}$. Assuming a rigid sphere collision, $\text{KrCl}(B)$ and $\text{KrCl}(C)$ experience 0.2 and 2.7 times collisions with He, respectively, within their radiative lifetimes at a He buffer gas pressure of 5 Torr. In the present study, the $B-X/C-A$ ratio increased from 2.0 to 4.7 with increasing the He buffer gas pressure from 1.5 to 5.5 Torr. On the basis of this finding, collisional relaxation takes place under operating conditions. Summarizing the above results, the $\text{KrCl}(B,C,D)$ excimers are formed from the fol-

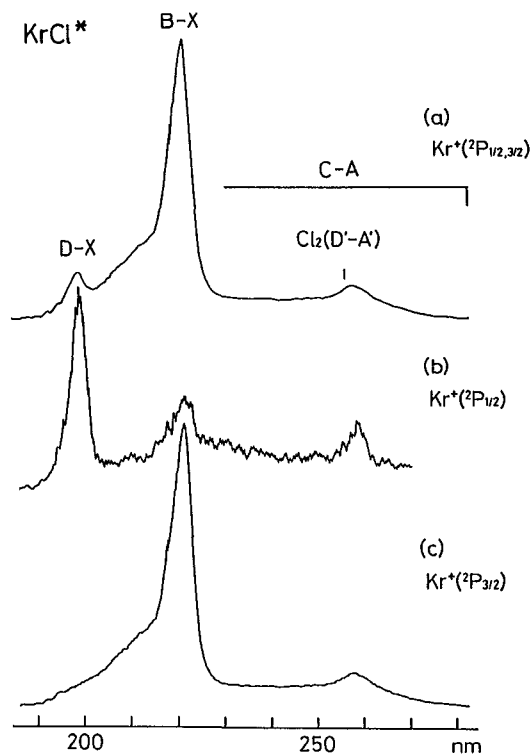
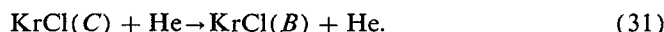
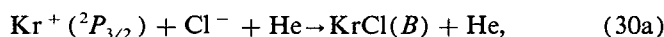


FIG. 6. KrCl^* emissions produced by the (a) $\text{Kr}^+ (^2P_{1/2,3/2}) + \text{Cl}^- + \text{He}$, (b) $\text{Kr}^+ (^2P_{1/2}) + \text{Cl}^- + \text{He}$, and (c) $\text{Kr}^+ (^2P_{3/2}) + \text{Cl}^- + \text{He}$ reactions in the He afterglow at a He pressure of 5 Torr (uncorrected for spectral response). Optical resolution was 4.7 \AA .

lowing excitation and relaxation processes under the present experimental conditions:



The branching fraction of $k_{29a}:k_{29c}$ was estimated to be $0.21 \pm 0.02:0.79 \pm 0.05$ from the integrated intensities of the $\text{KrCl}(B-X)$ and $\text{KrCl}(D-X)$ emissions. In the present study, low He pressure experiments below 1.5 Torr were difficult, though they are necessary to obtain the nascent $B-X/C-A$ ratio in the three-body reaction. The nascent $k_{29a}:k_{29b}$ and $k_{30a}:k_{30b}$ branching fractions were estimated by extrapolating the He pressure dependence of the $B-X/C-A$ ratio to the zero He pressure. The nascent $k_{29a}:k_{29b}$ and $k_{30a}:k_{30b}$ ratios thus obtained are $0.61 \pm 0.06:0.39 \pm 0.04$ and $0.60 \pm 0.06:0.40 \pm 0.04$, respectively.

Figures 7(a)–7(c) show the XeCl^* spectra obtained from the three-body ionic-recombination reactions by $\text{Xe}^+ (^2P_{1/2,3/2})$, $\text{Xe}^+ (^2P_{1/2})$, and $\text{Xe}^+ (^2P_{3/2})$, respectively. The most outstanding feature of the XeCl^* spectrum by the $\text{Xe}^+ (^2P_{1/2,3/2})$ reaction in comparison with the KrCl^*

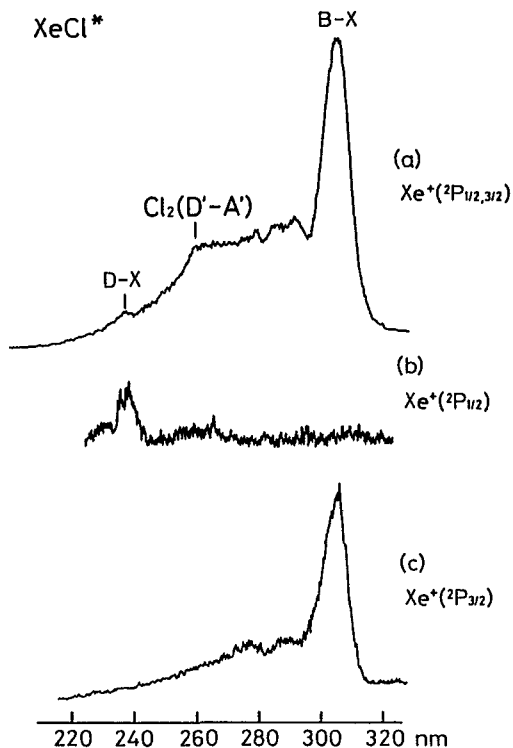
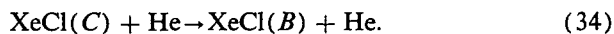
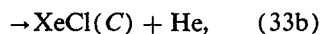
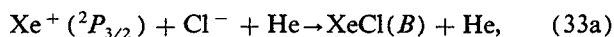
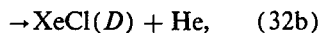
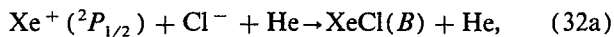


FIG. 7. XeCl* emissions produced by the (a) $\text{Xe}^+(^2P_{1/2,3/2}) + \text{Cl}^- + \text{He}$, (b) $\text{Xe}^+(^2P_{1/2}) + \text{Cl}^- + \text{He}$, and (c) $\text{Xe}^+(^2P_{3/2}) + \text{Cl}^- + \text{He}$ reactions in the He afterglow at a He pressure of 5 Torr (uncorrected for spectral response). Optical resolution was 4.7 Å,

spectrum by the $\text{Kr}^+(^2P_{1/2,3/2})$ reaction is that the intensity of the $D-X$ emission is very weak, relative to that of the $B-X$ emission. It should be noted that only $D-X$ is detected by the $\text{Xe}^+(^2P_{1/2})$ reaction. The upper limit of the $\text{XeCl}(B-X)/\text{XeCl}(D-X)$ ratio was estimated to be 0.08 from the signal-to-noise ratio. The $\text{Xe}^+(^2P_{3/2})$ reaction provides a strong $B-X$ transition and a weak continuous $C-A$ transition as in the $\text{Kr}^+(^2P_{3/2})$ reaction. Since the $B-X/C-A$ ratio in the $\text{Xe}^+(^2P_{3/2})$ reaction decreased from 5.0 to 2.0 upon reduction of the He pressure from 6.0 to 1.5 Torr, the electronic state transfer from C to B takes place even at the lowest He pressure of 1.5 Torr used to obtain a reliable $B-X/C-A$ ratio. Consequently, the $\text{XeCl}(B,C,D)$ excimers result from the following spin-orbit selective reactions and subsequent collisional relaxation under the operating conditions:



In order to obtain the nascent $k_{33a}:k_{33b}$ branching ratio, effects of collisional relaxation from C to B must be corrected. The τ_B and τ_C values were measured as 11.2 ± 0.2 and 131 ± 10 ns, respectively,⁴¹ and the separation between the B and C states is small ($\Delta E_{BC} = -90 \pm 2 \text{ cm}^{-1}$).²⁵ A simple gas kinetic model predicts that $\text{XeCl}(B)$ and $\text{XeCl}(C)$

collide with the buffer He gas 0.3 and 4.0 times, respectively, during their radiative lifetimes at a He pressure of 5 Torr. The collisional relaxation of $\text{XeCl}(B,C)$ by the buffer He atoms has been studied by Dreiling and Setser.¹⁹ According to their results, the $C \rightarrow B$ electronic energy transfer takes place below He pressure of 1.5 Torr. The nascent $k_{33a}:k_{33b}$ ratio was estimated to be $0.62 \pm 0.06:0.38 \pm 0.04$ by smoothly extrapolating the He pressure dependence of the $B-X/C-A$ ratio into the zero He pressure.

The spin-orbit state selectivity for the formation of each excimer state in the three-body ionic-recombination reactions is summarized in Table I along with the corresponding selectivity found in the two-body $\text{Rg}^+(^2P_{1/2,3/2})/\text{SF}_6^-$ and $\text{Rg}(^3P_{0,2})/\text{CCl}_4$ reactions. The B/C ratio for the $\text{Xe}(^3P_2)/\text{CCl}_4$ reaction obtained in the present study agrees well with that of Kolts *et al.*¹⁶ The B/C ratio by the $\text{Rg}(^3P_2)$ reaction increases from 0.49 to 1.6 in the $\text{Ar}(^3P_2)$, $\text{Kr}(^3P_2)$, $\text{Xe}(^3P_2)$ series. Extensive measurements for the $\text{Xe}(^3P_2)$ reactions with halogen donors giving XeCl^* have shown that the nascent B/C ratios generally are 1.4 ± 0.2 .¹⁶ Here we found that the nascent B/C ratio of XeCl^* is approximately the same for the $\text{Xe}^+(^2P_{3/2}) + \text{Cl}^- + \text{He}$ reaction ($B/C = 1.6$). The $\text{Kr}^+(^2P_{1/2}) + \text{Cl}^- + \text{He}$ and $\text{Kr}^+(^2P_{3/2}) + \text{Cl}^- + \text{He}$ reactions give a similar ratio of ~ 1.5 . This value is about 60% larger than that in the $\text{Kr}(^3P_2)/\text{CCl}_4$ reaction. We have recently shown in the two-body ionic-recombination reactions of $\text{Rg}^+(^2P_{1/2,3/2})/\text{SF}_6^-$ that there are propensities for the formation of D in the $\text{Rg}^+(^2P_{1/2})$ reaction and for the formation of B and C in the $\text{Rg}^+(^2P_{3/2})$ reaction.⁷ Here, it was demonstrated that a similar high spin-orbit state selectivity is conserved in the three-body ionic-recombination reactions $\text{Rg}^+(^2P_{1/2,3/2}) + \text{Cl}^- + \text{He}$ for Kr^+ and Xe^+ . In the all $\text{Rg}^+(^2P_{3/2})$ reactions, only B and C states are produced with B/C ratios of 1.5–2.1. On the other hand, the B , C , and D states are formed by the $\text{Rg}^+(^2P_{1/2})$ reaction and the $D/(B+C)$ ratio depends upon the reaction system. The D/B ratio is nearly equal for the $\text{Kr}^+(^2P_{1/2})/\text{SF}_6^-$ and $\text{Xe}^+(^2P_{1/2})/\text{SF}_6^-$ two-body reactions, while a significant difference is found in the $D/(B+C)$ selectivity between the $\text{Kr}^+(^2P_{1/2}) + \text{Cl}^- + \text{He}$ and $\text{Xe}^+(^2P_{1/2}) + \text{Cl}^- + \text{He}$ three-body reactions.

The formation of RgCl^* excimers proceeds through the approach of an Rg^+ and Cl^- ion pair under their mutual Coulombic field followed by deactivation of the ion pair by collision with the third-body He atom. Assuming that the He atom acts only an energy acceptor, potential energies of $\text{Rg}^+ + \text{Cl}^- + \text{He}$ are not perturbed by the He atom. According to theoretical calculations on rare gas monohalides by Dunning and Hay,^{24,27,28} the B and C states of RgCl^* are diabatically correlated to the $\text{Rg}^+(^2P_{3/2}) + \text{Cl}^-$ ion pair, whereas the D state dissociates to $\text{Rg}^+(^2P_{1/2}) + \text{Cl}^-$. Figures 8 and 9 show potential energy diagrams of $\text{KrCl}(B,C,D)$ and $\text{XeCl}(B,C,D)$, respectively. Figure 8 is drawn assuming that the potential curves of KrCl^* are the same as those of XeCl^* except for their relative energies. The preferential formation of D from the $\text{Rg}^+(^2P_{1/2})$ reaction and the selective formation of B and C from the $\text{Rg}^+(^2P_{3/2})$ reaction suggest that the $\text{Rg}^+(^2P_{1/2}) + \text{Cl}^-$ and Rg^+

TABLE I. Branching fractions of RgX* excimers.

	Reaction system	Branching fraction of RgX(B,C,D)		
		Γ_B	Γ_C	Γ_D
Sadeghi <i>et al.</i> ^a	Ar(³ P ₀) + CCl ₄	0.19 (0.26)	~0.07 (~0.08)	0.74 (0.66)
	Ar(³ P ₂) + CCl ₄	0.33	0.67	
This work	Kr(² P _{1/2}) + Cl ⁻ + He	0.19 ± 0.02	0.12 ± 0.01	0.69 ± 0.04
	Kr(² P _{3/2}) + Cl ⁻ + He	0.60 ± 0.06	0.40 ± 0.04	
Tsuji <i>et al.</i> ^b	Kr(² P _{1/2}) + SF ₆	0.05		0.95
	Kr(² P _{3/2}) + SF ₆	0.62	0.38	
This work ^c	Kr(³ P ₂) + CCl ₄	0.48 ± 0.05	0.52 ± 0.05	
This work	Xe(² P _{1/2}) + Cl ⁻ + He	≤ 0.07		≥ 0.93
	Xe(² P _{3/2}) + Cl ⁻ + He	0.62 ± 0.06	0.38 ± 0.04	
Tsuji <i>et al.</i> ^b	Xe(² P _{1/2}) + SF ₆	0.06		0.94
	Xe(² P _{3/2}) + SF ₆	0.68	0.32	
Kolts <i>et al.</i> ^d	Xe(³ P ₂) + CCl ₄	0.60 (0.55)	0.40 (0.45)	
This work ^e	Xe(³ P ₂) + CCl ₄	0.62 ± 0.06	0.38 ± 0.04	

^a Reference 20. Values in parentheses are obtained from data in Table II, which are different from those in Table I.

^b Reference 7.

^c Ratios were obtained at a Kr pressure of 35 mTorr.

^d Reference 16. Ratios are from spectra taken at 0.09 to 0.15 Torr. Values in parentheses are zero pressure extrapolated limit.

^e Ratios were obtained at an Ar pressure of 0.1 Torr.

(²P_{3/2}) + Cl⁻ characters are generally conserved in the three-body reaction of Rg⁺(²P_{1/2,3/2}) + Cl⁻ + He. This means that the third-body He atom acts as only energy acceptor and relaxation from the entrance Rg⁺(²P_{1/2}) + Cl⁻ potential to the Rg⁺(²P_{3/2}) + Cl⁻ potential by collisions with the third-body He atom is not so efficient. For the ex-

cimer formation, the attractive ion-pair potentials must pass through a number of Rg* + Cl and Rg + Cl* covalent-potential crossings. If the ion-pair potentials strongly couple with some of these covalent potentials, this coupling will divert trajectories from the ion-pair potentials to products correlating to the neutral fragments. The preferential forma-

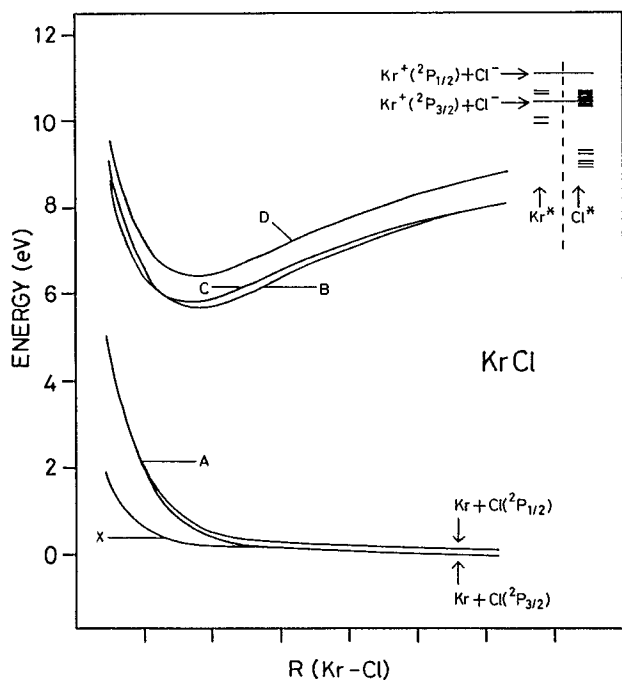


FIG. 8. Potential diagram for KrCl. The potentials were sketched from analogy to the XeCl potentials of Ref. 24. Low-lying state of Kr*, Kr⁺, and Cl* are shown to the right. The ion-pair energies, Kr⁺(²P_{1/2,3/2}) + Cl⁻, are indicated by the two longer lines; the B and C curves go to the lower of these and the D curve to the upper.

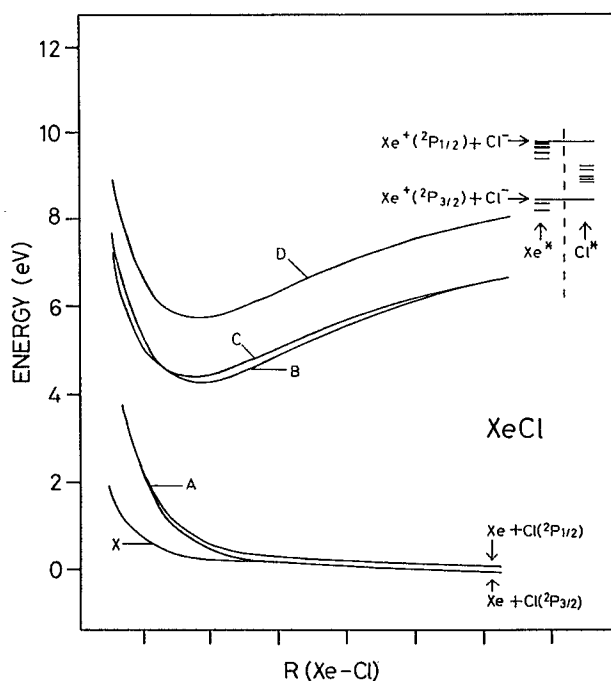


FIG. 9. Potential diagram for XeCl and atomic Xe* and Cl*. The XeCl potentials were sketched from the information in Ref. 24. The B and C curves are correlated to the lower Xe⁺(²P_{3/2}) + Cl⁻ ion pair and the D curve to the upper Xe⁺(²P_{1/2}) + Cl⁻ one.

tion of D by the $\text{Rg}^+ (^2P_{1/2})$ reactions and the selective formation of B and C by the $\text{Rg}^+ (^2P_{3/2})$ reactions imply that there are diabatically passes to form RgCl^* from the ion-pair potentials, even though many $\text{Rg}^* + \text{Cl}$ and $\text{Rg} + \text{Cl}^*$ potentials are present and some of them can strongly interact with the entrance ion-pair potentials.

The formation of $\text{KrCl}(B,C)$ in processes (29a) and (29b) suggests that an energy transfer takes place from the upper $\text{Kr}^+ (^2P_{1/2}) + \text{Cl}^-$ potential to the lower $\text{Kr}^+ (^2P_{3/2}) + \text{Cl}^-$ one. There are two possible processes for the formation of $\text{KrCl}(B,C)$ by the $\text{Kr}^+ (^2P_{1/2}) + \text{Cl}^-$ reaction. One is collisional transfer by the third-body He atom from $[\text{Kr}^+ (^2P_{1/2})\text{Cl}^-]^*$ to $[\text{Kr}^+ (^2P_{3/2})\text{Cl}^-]^*$. The other is intramolecular energy transfer from $[\text{Kr}^+ (^2P_{1/2})\text{Cl}^-]^*$ to $[\text{Kr}^+ (^2P_{3/2})\text{Cl}^-]^*$ through another potential which intersects both potentials. Possible potentials are $\text{Kr}^+ + \text{Cl}^-$, $\text{Kr}^* + \text{Cl}$, and $\text{Kr} + \text{Cl}^*$, which can couple with both the upper and lower ion-pair potentials. The predissociation mechanism could also be involved in the latter process for the $\text{KrCl}(B,C)$ formation from $[\text{Kr}^+ (^2P_{1/2})\text{Cl}^-]^*$. If trajectories leave the $\text{KrCl}(D)$ potential as $\text{Kr}^* + \text{Cl}$ or $\text{Kr} + \text{Cl}^*$ and if these trajectories are diverted back to $\text{KrCl}(B,C)$ at long range from the $\text{Kr}^+ (^2P_{3/2})\text{Cl}^-$ potential, then $\text{KrCl}(B,C)$ will be produced. A similar breakdown of $\text{Rg}^+ (^2P_{1/2}) + \text{X}^-$ character has been found in the two-body $\text{Rg}^+ (^2P_{1/2})/\text{SF}_6^-$ ionic-recombination reaction, in which the formation of the B state must proceed through the latter intramolecular energy transfer from $[\text{Rg}^+ (^2P_{1/2})\text{SF}_6^-]^*$ to $[\text{Rg}^+ (^2P_{3/2})\text{SF}_6^-]^*$.⁷ It may therefore, be reasonable to assume that the intramolecular process as well as the collisional transfer process takes part in the formation of $\text{KrCl}(B,C)$ in the three-body reaction. One reason for the low $\text{XeCl}(B)$ yield from the $\text{Xe}^+ (^2P_{1/2}) + \text{Cl}^- + \text{He}$ reaction is a large ΔE_{BD} separation of 1.24 eV which will reduce the possibility of such a collisional transfer process. As shown later, if $\text{XeCl}(B)$ is produced by the three-body reaction, the $\text{XeCl}(B)$ formation must compete with both the $\text{XeCl}(D)$ formation and predissociation of $[\text{Xe}^+ (^2P_{1/2})\text{Cl}^-]^*$. Thus the other reason for the low $\text{XeCl}(B)$ yield is competition of fast predissociation of $[\text{Xe}^+ (^2P_{1/2})\text{Cl}^-]^*$ into $\text{Xe}^* + \text{Cl}$ and/or $\text{Xe} + \text{Cl}^*$.

The spin-orbit state selectivity for the excimer formation in reactions of metastable $\text{Rg} (^3P_{2,0})$ atoms with halogen-containing molecules has been studied by Golde and Poletti²¹ and Setser and his co-workers.^{20,42} It was found that $\text{Rg} (^3P_2)$ atoms give only the B and C states, while $\text{Rg} (^3P_0)$ atoms give a mixture of B, C , and D states with B and D being favored. These results have been generally explained by the conservation of the Rg^+ ion-core configuration during the reaction; $\text{Rg} (^3P_2)$ atoms would be expected to form $\text{Rg}^+ (^2P_{3/2})\text{X}^-$ ionic products in the B and C states, whereas $\text{Rg} (^3P_0)$ atoms should yield the D state through an $[\text{Rg}^+ (^2P_{1/2})\text{X}^-]^*$ intermediate. The formation of B and C from the $\text{Rg} (^3P_0)$ reaction, which does not conserve the ion-core configuration, was explained by a crossing between the $\Omega = 0^-$ entrance channel potential from $\text{Rg} (^3P_0)$ with an $\Omega = 0^-$ potential arising from $\text{Rg}^+ (^2P_{3/2}) + \text{X}^-$. The de-

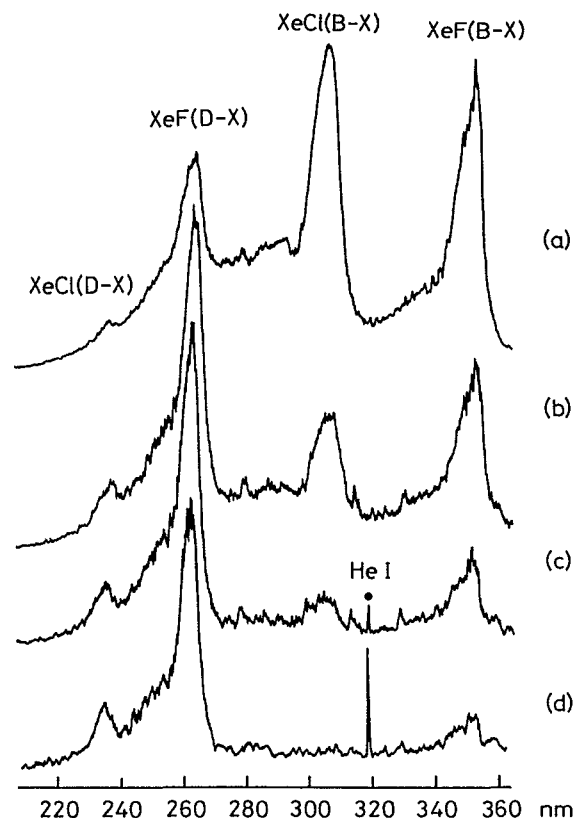


FIG. 10. A comparison of XeCl^* and XeF^* emissions resulting from the $\text{Xe}^+ (^2P_{1/2,3/2}) + \text{Cl}^- + \text{He}$ and $\text{Xe}^+ (^2P_{1/2,3/2})\text{SF}_6$ reactions at $[\text{Xe}^+ (^2P_{1/2})]:[\text{Xe}^+ (^2P_{3/2})]$ ratios of 1:1, 5:1, 9:1, and 1:0 for (a)–(d), respectively (uncorrected for spectral response). The spectra were measured at a He buffer gas pressure of 4.5 Torr with optical resolution of 4.7 Å.

gree of the $D/(B + C)$ selectivity in the $\text{Ar} (^3P_0)$ reactions with various halogen donors has been measured as 0.53–2.8.²⁰ In the $\text{Rg} (^3P_0) + \text{RX}$ reactions, the crossing between the two $\Omega = 0^-$ potentials must occur before the formation of the $[\text{Rg}^+ (^2P_{1/2})\text{RX}^-]$ intermediate. Since such a crossing is unnecessary in the ionic-recombination reactions, a higher propensity for the formation of $\text{RgX}(D)$ can generally be achieved.

C. Relative formation rate constants of $\text{RgCl}(B,C)$ and $\text{RgCl}(D)$

In order to examine the relative formation rate constant of $\text{RgCl}(D-X)$ from the $\text{Rg}^+ (^2P_{1/2})$ reaction and $\text{RgCl}(B-X, C-A)$ from the $\text{Rg}^+ (^2P_{3/2})$ reaction, RgCl^* emissions from the three-body reactions are compared with RgF^* emissions from the $\text{Rg}^+ / \text{SF}_6^-$ reactions by using a 1:10 mixture of $\text{SF}_6:\text{CCl}_4$ as a reagent. As an example, Fig. 10 shows $\text{XeCl}(B-X, D-X)$ and $\text{XeF}(B-X, D-X)$ emissions obtained at various $[\text{Xe}^+ (^2P_{1/2})]/[\text{Xe}^+ (^2P_{3/2})]$ ratios. At the lowest $[\text{Xe}^+ (^2P_{1/2})]/[\text{Xe}^+ (^2P_{3/2})]$ ratio of 1:1 [Fig. 10(a)], the $\text{XeCl}(B-X)$ and $\text{XeF}(B-X)$ emissions are dominant. With increasing the $[\text{Xe}^+ (^2P_{1/2})]/[\text{Xe}^+ (^2P_{3/2})]$ ratio by addition of the filter O_2 gas, the

XeCl(*D-X*) and XeF(*D-X*) emissions are enhanced and the XeCl(*B-X*) emission finally disappears. A significant difference in the *B-X/D-X* ratio is found between the XeF* and XeCl* emissions, indicating that a large difference is present in the $k_{RgX(D)}/k_{RgX(B)}$ ratio between the two-body and three-body ionic-recombination reactions. When SF₆ was introduced from a few mm downstream from the Xe gas inlet in order to obtain a nascent intensity ratio between XeF(*D-X*) from Xe⁺(²P_{1/2})/SF₆⁻ and XeF(*B-X*) from Xe⁺(²P_{3/2})/SF₆⁻, the *B-X/D-X* ratio was ~2. This result, coupled with that fact the [Xe⁺(²P_{3/2})]/[Xe⁺(²P_{1/2})] ratio formed in the He(²S)/Xe Penning ionization is ~2, suggests that there is no significant difference between the formation rate constant of XeF(*D-X*) from Xe⁺(²P_{1/2})/SF₆⁻ and that of XeF(*B-X*) from Xe⁺(²P_{3/2})/SF₆⁻. Similar results have been obtained for KrCl* and KrF* emissions. Assuming that the formation rate constants of RgF(*D-X*) from Rg⁺(²P_{1/2})/SF₆⁻ are the same as those of RgF(*B-X*) from Rg⁺(²P_{3/2})/SF₆⁻, the relative formation rate constants of RgCl(*B-X*) and RgCl(*D-X*) in the three-body ionic-recombination reactions are evaluated. The k_{29c}/k_{30a} and k_{32b}/k_{33a} ratios are estimated to be 0.23 ± 0.03 and 0.053 ± 0.010 , respectively, by comparing the integrated intensities of RgCl* emissions with those of RgF* emissions. These ratios and the nascent *B:C:D* distributions of RgCl* give $(k_{29a} + k_{29b} + k_{29c})/(k_{30a} + k_{30b}) = 0.20 \pm 0.03$, $k_{29c}/(k_{30a} + k_{30b}) = 0.14 \pm 0.02$, $(k_{32a} + k_{32b})/(k_{33a} + k_{33b}) = 0.033 \pm 0.06$ – 0.035 ± 0.06 , and $k_{32b}/(k_{33a} + k_{33b}) = 0.033 \pm 0.06$.

There are two possible reasons for the smaller formation rate constants of RgCl(*D*) from Rg⁺(²P_{1/2}) + Cl⁻ + He than those of RgCl(*B,C*) from Rg⁺(²P_{3/2}) + Cl⁻ + He. One is that the total rate constants of Rg⁺(²P_{1/2}) + Cl⁻ + He are smaller than those of Rg⁺(²P_{3/2}) + Cl⁻ + He. The other is that predissociation rates of [Rg⁺(²P_{1/2})Cl⁻]* into Rg* + Cl and/or Rg + Cl* are faster than those of [Rg⁺(²P_{3/2})Cl⁻]*. In order to examine the former contribution, various Rg/CCl₄ mixtures were introduced from the first gas inlet to form RgCl(*B,C,D*) excimers and a small amount of SF₆ was injected from the second gas inlet to monitor residual [Rg⁺(²P_{1/2})]/[Rg⁺(²P_{3/2})] ratio by observing the Rg⁺(²P_{1/2,3/2})/SF₆⁻ reactions. For example, Figs. 11(a) and 11(b) show the XeF(*B-X,D-X*) spectra observed without and with CCl₄ mixing, respectively. Although the XeF(*B-X,D-X*) emissions reduce their intensities by addition of CCl₄ by a factor of ~4 as shown in Fig. 11(b) due to quenching of Xe⁺(²P_{1/2,3/2}) by the three-body ionic-recombination reactions and the Xe⁺(²P_{1/2,3/2})/CCl₄ reactions, the XeF(*D-X*)/XeF(*B-X*) ratio is essentially identical. When the XeF(*B-X,D-X*) emissions from the Xe⁺(²P_{1/2,3/2})/SF₆⁻ reactions were measured by using various SF₆/CCl₄ mixtures, the *D-X/B-X* ratio was independent of the relative concentration of CCl₄. This implies that there is no significant difference in the total rate constants between the Xe⁺(²P_{1/2})/CCl₄ and Xe⁺(²P_{3/2})/CCl₄ reactions. On the basis of above findings, the total rate constants of Xe⁺(²P_{1/2}) + Cl⁻ + He and

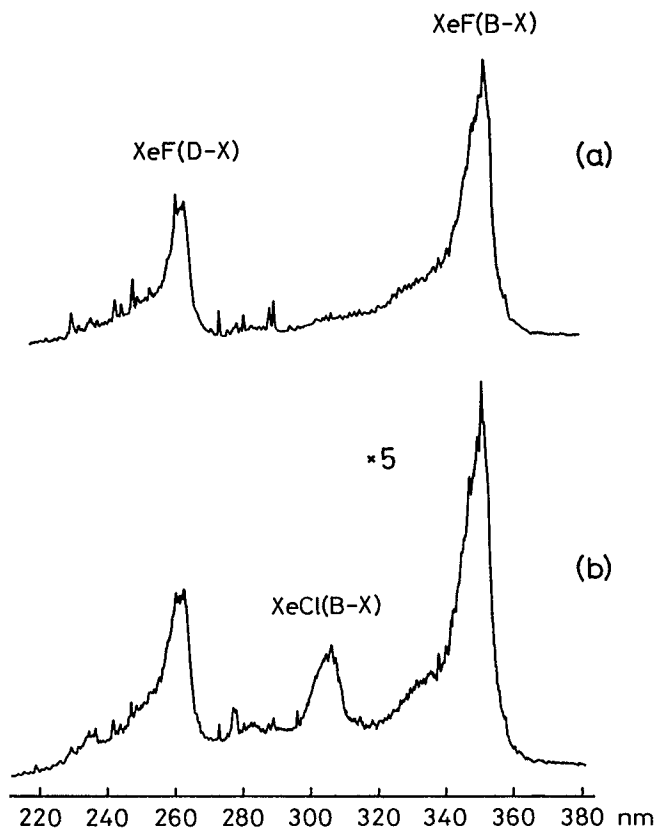


FIG. 11. XeF* emissions resulting from the Xe⁺(²P_{1/2,3/2}) + SF₆ reaction (a) without CCl₄ mixing and (b) with CCl₄ mixing from the first gas inlet at a He pressure of 1.3 Torr (uncorrected for spectral response). Optical resolution was 4.7 Å.

Xe⁺(²P_{3/2}) + Cl⁻ + He are nearly the same and the small XeCl(*D-X*)/XeCl(*B-X*) ratios are attributed to the fact that the entrance Xe⁺(²P_{1/2})Cl⁻ potential correlating to XeCl(*D*) suffers more loss via competition with predissociation than do the Xe⁺(²P_{3/2})Cl⁻ potentials correlating to XeCl(*B,C*). A similar result was obtained for the KrCl(*D-X*)/KrCl(*B-X*) ratio in the Kr⁺(²P_{1/2,3/2}) + Cl⁻ + He reactions. When emission spectra resulting from Rg⁺(²P_{1/2,3/2}) + Cl⁻ + He were observed in the 190–600 nm region, neither strong Rg* nor Cl* were detected. Therefore, it is reasonable to predict that most of Rg* and/or Cl* atoms produced through predissociation are located in either nonemitting states or emitting states outside the present observation region. The metastable Rg(³P_{2,0}) atoms can be removed from the possible candidates as shown in Sec. III A.

The formation rates of Rg* and Cl* must depend upon the crossing points of the ion pair (RgCl*) and relevant Rydberg (Rg* + Cl or Rg + Cl*) states and the strength of the coupling between each pair of states. Assuming that the Rg* + Cl and Rg + Cl* potentials are simply repulsive, 12 and 28 Kr(³P_{*J*}) + Cl(²P_{*J*}) and Kr(¹S₀) + Cl* potentials can intersect the KrCl(*B,C*) and KrCl(*D*) potentials, respectively, whereas three Xe(³P_{2,1}) + Cl(²P_{*J*}) and 19 Xe(³P_{*J*}) + Cl(²P_{*J*}), Xe(¹S₀) + Cl*, and Xe(*6p*)

+ Cl(2P_J) potentials can cross the XeCl(B,C) and XeCl(D) potentials, respectively (see Figs. 8 and 9). The crossing points for the formation of Rg* and Cl* occur at shorter internuclear distances for RgCl(D); hence, the strength of the interactions is stronger. Since more predissociation channels are open and the interactions between the ion-pair potential and the dissociative Rydberg potentials are stronger for the upper RgCl(D) potentials, the predissociation rates of $[\text{Rg}^+(\text{}^2P_{1/2})\text{Cl}^-]^*$ will be faster than those of $[\text{Rg}^+(\text{}^2P_{3/2})\text{Cl}^-]^*$. This is consistent with the lower RgCl(D) yields from $\text{Rg}^+(\text{}^2P_{1/2}) + \text{Cl}^- + \text{He}$ than the RgCl(B,C) yields from $\text{Rg}^+(\text{}^2P_{3/2}) + \text{Cl}^- + \text{He}$. The difference in the predissociation rate will be enhanced with increasing the ΔE_{BD} value ($\Delta E_{BD} \sim 0.7$ eV for KrCl* and 1.24 eV for XeCl*), because the difference in the number of predissociation channels becomes large. This can explain the present observation that the relative formation rate constant of XeCl(D) from $\text{Xe}^+(\text{}^2P_{1/2}) + \text{Cl}^- + \text{He}$ to that of XeCl(B,C) from $\text{Xe}^+(\text{}^2P_{3/2}) + \text{Cl}^- + \text{He}$ is smaller than that for KrCl* by a factor of 4.2.

D. Summary

Appropriate filter gases were used to prepare one of the spin-orbit states of $\text{Rg}^+(\text{}^2P_{1/2,3/2})$ in the flowing afterglow. The spin-orbit state selectivity was studied for the three-body ionic-recombination reactions of $\text{Rg}^+(\text{}^2P_{1/2,3/2}) + \text{Cl}^- + \text{He}$. The KrCl* and XeCl* product state distributions from the two spin-orbit states show a propensity for the $D(\Omega = 1/2)$ state formation by $\text{Rg}^+(\text{}^2P_{1/2})$; the $\text{Rg}^+(\text{}^2P_{3/2})$ reactions give only the $B(\Omega = 1/2)$ and $C(\Omega = 3/2)$ state products. These selectivities have been explained by conservation of $\text{Rg}^+(\text{}^2P_{1/2}) + \text{Cl}^-$ and $\text{Rg}^+(\text{}^2P_{3/2}) + \text{Cl}^-$ characters. The degree of conservation of spin-orbit state selectivity depended upon the reaction system. A high conservation of $\text{Rg}^+(\text{}^2P_{1/2,3/2}) + \text{Cl}^-$ characters was found for the D state formation by $\text{Xe}^+(\text{}^2P_{1/2}) + \text{Cl}^- + \text{He}$ and for the B and C state formation by $\text{Rg}^+(\text{}^2P_{3/2}) + \text{Cl}^- + \text{He}$ for both Kr^+ and Xe^+ . Meanwhile, a breakdown of the $\text{Kr}^+(\text{}^2P_{1/2}) + \text{Cl}^-$ character was found for the $\text{Kr}^+(\text{}^2P_{1/2}) + \text{Cl}^- + \text{He}$ reaction. It was attributed to collisional transfer from the $\text{Kr}^+(\text{}^2P_{1/2})\text{Cl}^-$ potential to the $\text{Kr}^+(\text{}^2P_{3/2})\text{Cl}^-$ one and/or intramolecular energy transfer from the $\text{Kr}^+(\text{}^2P_{1/2})\text{Cl}^-$ potential to the $\text{Kr}^+(\text{}^2P_{3/2})\text{Cl}^-$ one. The relative formation rate constants of RgCl(D) from $\text{Rg}^+(\text{}^2P_{1/2}) + \text{Cl}^- + \text{He}$ to those of RgCl(B,C) from $\text{Rg}^+(\text{}^2P_{3/2}) + \text{Cl}^- + \text{He}$ were estimated by reference to RgF($B-X, D-X$) emissions from $\text{Rg}^+(\text{}^2P_{1/2,3/2})/\text{SF}_6^-$. The $k_{\text{KrCl}(D)}/k_{\text{KrCl}(B,C)}$ ratio in the $\text{Kr}^+(\text{}^2P_{1/2,3/2}) + \text{Cl}^- + \text{He}$ reaction, 0.14 ± 0.02 , was larger than the $k_{\text{XeCl}(D)}/k_{\text{XeCl}(B,C)}$ one in the $\text{Xe}^+(\text{}^2P_{1/2,3/2}) + \text{Cl}^- + \text{He}$ reaction, 0.033 ± 0.006 . The smaller ratio in the latter reaction was interpreted as due to faster predissociation of $[\text{Xe}^+(\text{}^2P_{1/2})\text{Cl}^-]^*$ into $\text{Xe}^* + \text{Cl}$ and/or $\text{Xe} + \text{Cl}^*$ than that of $[\text{Kr}^+(\text{}^2P_{1/2})\text{Cl}^-]^*$ into $\text{Kr}^* + \text{Cl}$ and/or $\text{Kr} + \text{Cl}^*$.

ACKNOWLEDGMENTS

The authors wish to express their thanks to Professor D. W. Setser for his valuable correspondence. This work was supported by a Grand-in-Aid for Scientific Research from the Ministry of Education, Science, and Culture (No. 02640371), the Asahi Glass Foundation, and the Ito Science Foundation.

- ¹M. Rokni, J. H. Jacob, J. A. Mangano, and R. Brochu, *Appl. Phys. Lett.* **30**, 458 (1977).
- ²M. Rokni, J. H. Jacob, and J. A. Mangano, *Phys. Rev. A* **16**, 2216 (1977).
- ³M. Maeda, T. Nishitarumizu, and Y. Miyazoe, *Jpn. J. Appl. Phys.* **18**, 439 (1979).
- ⁴W. L. Nighan and R. T. Brown, *Appl. Phys. Lett.* **36**, 498 (1980).
- ⁵T. H. Johnson and A. M. Hunter, *J. Appl. Phys.* **51**, 2406 (1980).
- ⁶M. Tsuji, M. Furusawa, and Y. Nishimura, *Chem. Phys. Lett.* **166**, 363 (1990).
- ⁷M. Tsuji, M. Furusawa, and Y. Nishimura, *J. Chem. Phys.* **92**, 6502 (1990).
- ⁸A. J. Yencha, In *Electron Spectroscopy, Theory, Techniques, and Applications*, edited by C. R. Brundle and A. D. Baker (Academic, New York, 1984), Vol. 5, p. 197.
- ⁹C. E. Brion, C. A. McDowell, and W. B. Stewart, *J. Electron Spectrosc.* **1**, 113 (1972/73).
- ¹⁰F. C. Fehsenfeld, E. E. Ferguson, and A. L. Schmeltekopf, *J. Chem. Phys.* **45**, 404 (1966).
- ¹¹N. G. Adams, D. K. Bohme, D. B. Dunkin, and F. C. Fehsenfeld, *J. Chem. Phys.* **52**, 1951 (1970).
- ¹²D. Smith and N. G. Adams, *Phys. Rev. A* **23**, 2327 (1981).
- ¹³D. M. Sonnenfroh and S. R. Leone, *J. Chem. Phys.* **90**, 1677 (1989).
- ¹⁴K. Giles, N. G. Adams, and D. Smith, *J. Phys. B* **22**, 873 (1989).
- ¹⁵L. A. Gundel, D. W. Setser, M. A. A. Clyne, J. A. Coxon, and W. Nip, *J. Chem. Phys.* **64**, 4390 (1976).
- ¹⁶J. H. Kolts, J. E. Velazco, and D. W. Setser, *J. Chem. Phys.* **71**, 1247 (1979).
- ¹⁷K. Tamagake, J. H. Kolts, and D. W. Setser, *J. Chem. Phys.* **71**, 1264 (1979).
- ¹⁸D. W. Setser, T. D. Dreiling, H. C. Brashears, Jr., and J. H. Kolts, *Faraday Discuss. Chem. Soc.* **67**, 255 (1979).
- ¹⁹T. D. Dreiling and D. W. Setser, *J. Chem. Phys.* **75**, 4360 (1981).
- ²⁰N. Sadeghi, M. Cheaib, and D. W. Setser, *J. Chem. Phys.* **90**, 219 (1989).
- ²¹M. F. Golde and R. A. Poletti, *Chem. Phys. Lett.* **80**, 23 (1981).
- ²²V. E. Velazco, J. H. Kolts, and D. W. Setser, *J. Chem. Phys.* **65**, 3468 (1976).
- ²³H. M. Rosenstock, K. Draxl, G. W. Steiner, and J. T. Herron, *J. Phys. Chem. Ref. Data* **6**, Suppl. No. 1 (1977).
- ²⁴P. J. Hay and T. H. Dunning Jr., *J. Chem. Phys.* **69**, 2209 (1978).
- ²⁵C. Jouvet, C. Lardeux-Dedonder, and D. Solgadi, *Chem. Phys. Lett.* **156**, 569 (1989).
- ²⁶Y. C. Yu and D. W. Setser, *J. Phys. Chem.* **94**, 2934 (1990).
- ²⁷T. H. Dunning, Jr. and P. J. Hay, *J. Chem. Phys.* **69**, 134 (1978).
- ²⁸P. J. Hay, W. R. Wadt, and T. H. Dunning, Jr., *Annu. Rev. Phys. Chem.* **30**, 311 (1979).
- ²⁹D. Smith, N. G. Adams, and E. Alge, *J. Phys. B* **17**, 461 (1984).
- ³⁰R. Cooper, L. S. Denison, P. Zeglinski, C. R. Roy, and H. Gillis, *J. Appl. Phys.* **54**, 3053 (1983).
- ³¹M. J. Church and D. Smith, *J. Phys. D* **11**, 2199 (1978).
- ³²M. R. Flannery and T. P. Yang, *Appl. Phys. Lett.* **32**, 327 (1978).
- ³³J. M. Wadehra and J. N. Bardsley, *Appl. Phys. Lett.* **32**, 76 (1978).
- ³⁴N. Sadeghi and D. W. Setser, *Chem. Phys. Lett.* **82**, 44 (1981).
- ³⁵M. Tsuji, K. Yamaguchi, and Y. Nishimura, *J. Chem. Phys.* **89**, 3391 (1988).
- ³⁶T. D. Nguyen, N. Sadeghi, and J. C. Pebay-Peyroula, *Chem. Phys. Lett.* **29**, 242 (1974).
- ³⁷J. Bel Bruno and J. Krenos, *Chem. Phys. Lett.* **74**, 430 (1980).
- ³⁸T. Krümpelmann and Ch. Ottinger, *Chem. Phys. Lett.* **140**, 142 (1987).
- ³⁹P. J. Dagdigian and M. L. Campbell, *Chem. Rev.* **87**, 1 (1987).
- ⁴⁰N. W. Winter, Lawrence Livermore Laboratory Report (1977).
- ⁴¹G. Inoue, J. K. Ku, and D. W. Setser, *J. Chem. Phys.* **80**, 6006 (1984).
- ⁴²R. Sobczynski, R. Beaman, D. W. Setser, and N. Sadeghi, *Chem. Phys. Lett.* **154**, 349 (1989).